SUPPLEMENTARY MATERIAL

Computational modeling highlights the role of the disordered Formin Homology 1 domain in profilin-actin transfer

Brandon G. Horan[1] | Gül H. Zerze[2] | Young C. Kim[3] | Dimitrios Vavylonis[1] | Jeetain Mittal[2]

1 Department of Physics, Lehigh University, Bethlehem, PA, 18015, USA
2 Department of Chemical and Biomolecular Engineering, Lehigh University, Bethlehem, PA, 18015, USA
3 Center for Materials Physics and Technology, Naval Research Laboratory, Washington, DC, 20375, USA

Movie Captions:

Movie 1: AA simulation of mDia1-FH1(6PRM) at 15fps. Each frame 1.5ns simulation time.

Movie 2: AA simulation of mDia2-FH1 at 15fps. Each frame 1.5ns simulation time.

Movie 3: AA simulation of Bni1-FH1 at 15fps. Each frame 1.5ns simulation time.

Movie 4: AA simulation of Bnr1-FH1 at 15fps. Each frame 1.5ns simulation time.

Movie 5: AA simulation of Cdc12-FH1 at 15fps. Each frame 1.5ns simulation time.

Movie 6: AA simulation of Fus1-FH1 at 15fps. Each frame 1.5ns simulation time.

Movie 7: AA simulation of For3-FH1 at 15fps. Each frame 1.5ns simulation time.

Movie 8: CG simulation of mDia1-FH1(6PRM) at 15fps. Each frame 10ns LAMMPS simulation time.

Movie 9: CG simulation of mDia2-FH1 at 15fps. Each frame 10ns LAMMPS simulation time.

Movie 10: CG simulation of Bni1-FH1 at 15fps. Each frame 10ns LAMMPS simulation time.

Movie 11: CG simulation of Bnr1-FH1 at 15fps. Each frame 10ns LAMMPS simulation time.

Movie 12: CG simulation of Cdc12-FH1 at 15fps. Each frame 10ns LAMMPS simulation time.

Movie 13: CG simulation of Fus1-FH1 at 15fps. Each frame 10ns LAMMPS simulation time.

Movie 14: CG simulation of For3-FH1 at 15fps. Each frame 10ns LAMMPS simulation time.

Movie 15: CG simulation of mDia1-FH1(6PRM) with profilin occupying two PRMs at 15fps. Each frame 10ns LAMMPS simulation time.

Movie 16: CG simulation of mDia1-FH1(6PRM) with profilin-actin occupying four PRMs at 15fps. Each frame 10ns LAMMPS simulation time.

Movie 17: CG simulation of Bni1-FH1-FH2 bound barbed end at 15 fps. Each frame 10ns LAMMPS. For convenience, barbed end is kept still in the movie.

Movie 18: Same as Movie 17, but a top view.

Movie 19: CG simulation of Bni1-FH1-FH2 bound barbed end at 30fps. Each frame 2ns. For convenience, barbed end is kept still in the movie. The incoming actin subunit associates transiently with the barbed end and dissociates from it at later times.

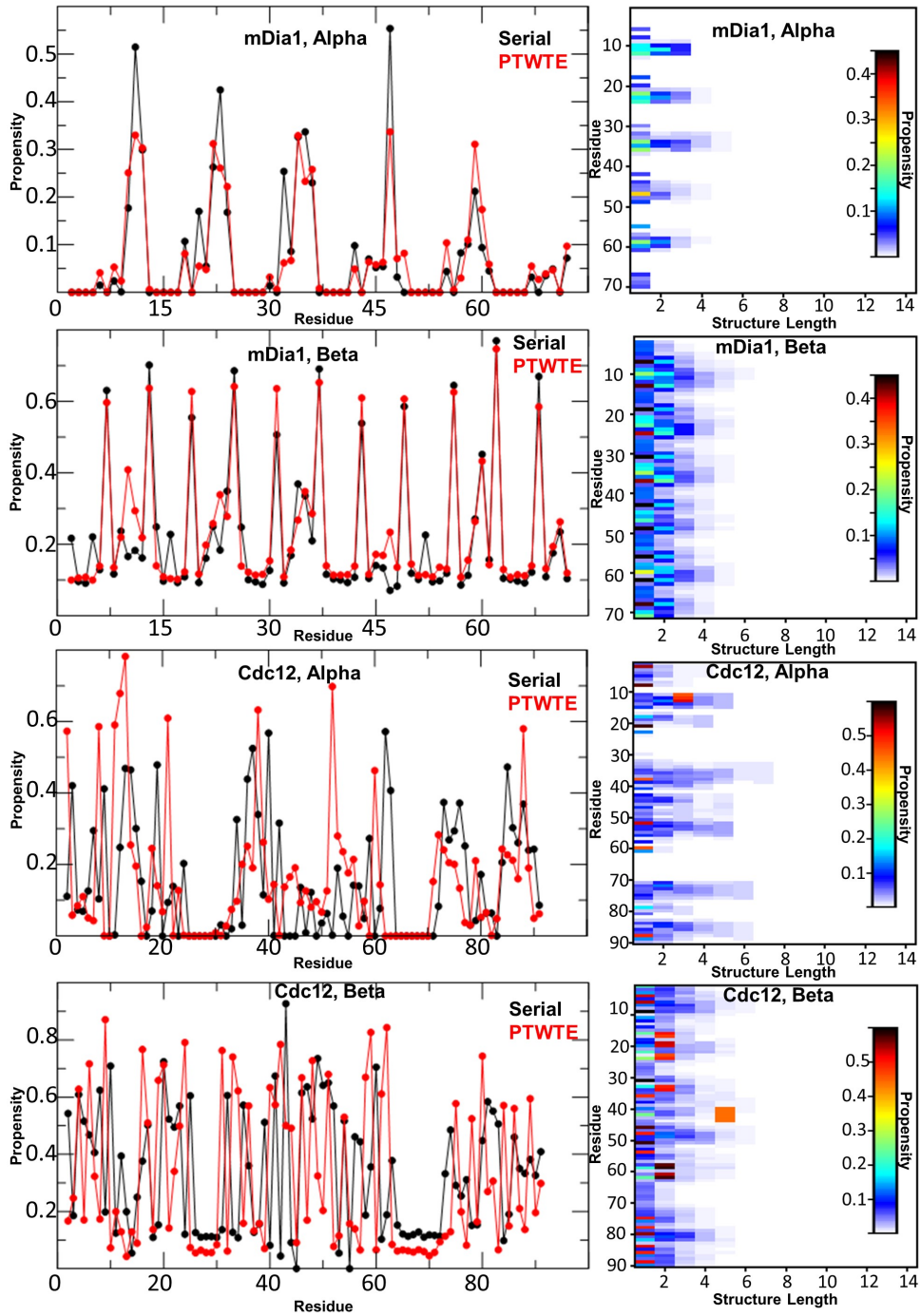

FIGURE S1 All-atom PTWTE simulations reveal little to no alpha or beta type structures in the FH1 domains shown in Fig. 1A of the main text. Secondary structure is classified by backbone dihedral angles.

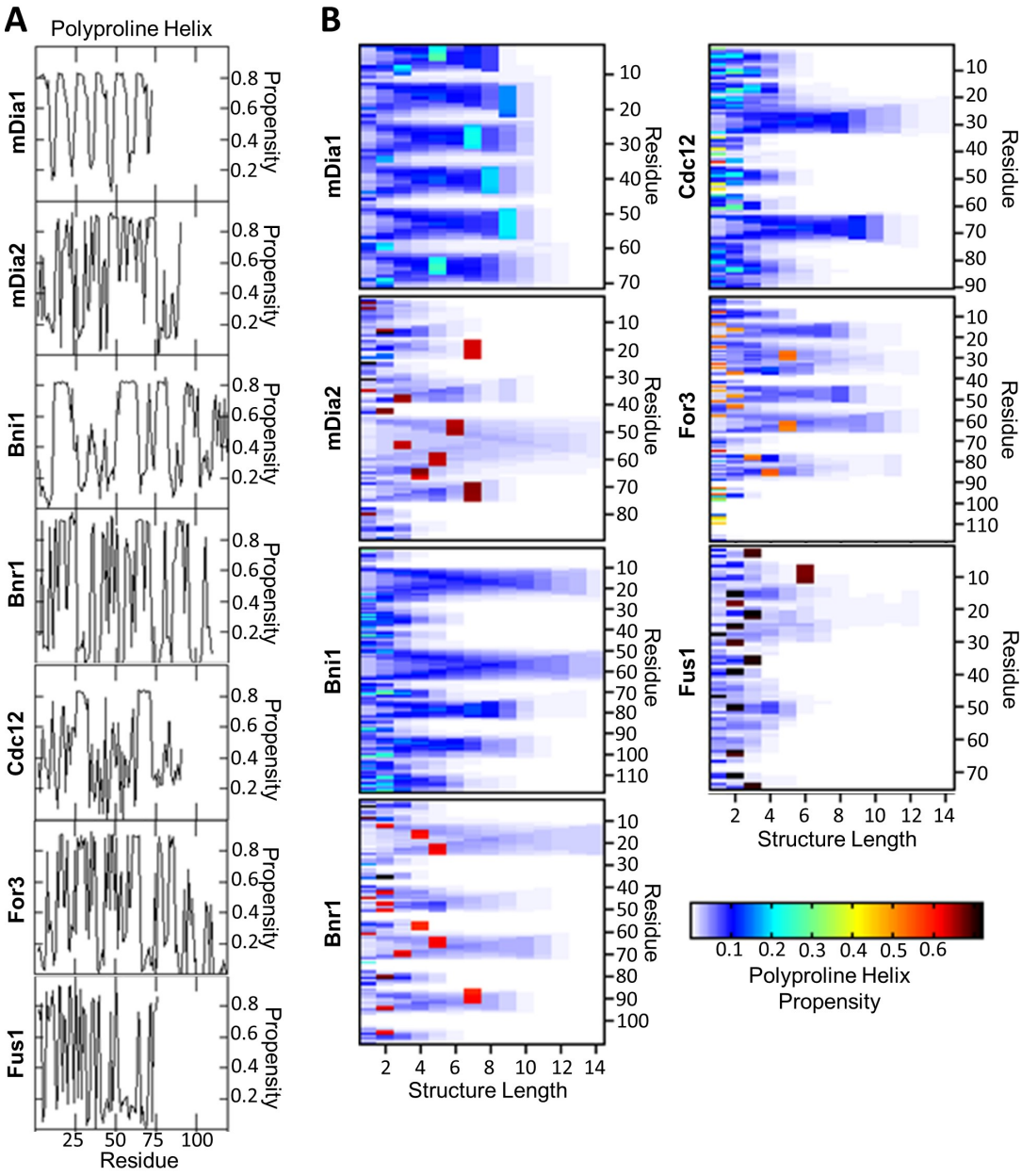

FIGURE S2 **All-atom serial simulations reveal PP helices in the FH1 domains of Fig. 1A of the main text. A**: Total per-residue propensity. **B**: Per-residue and structure length propensity for polyproline helix. Secondary structure is classified by backbone dihedral angles.

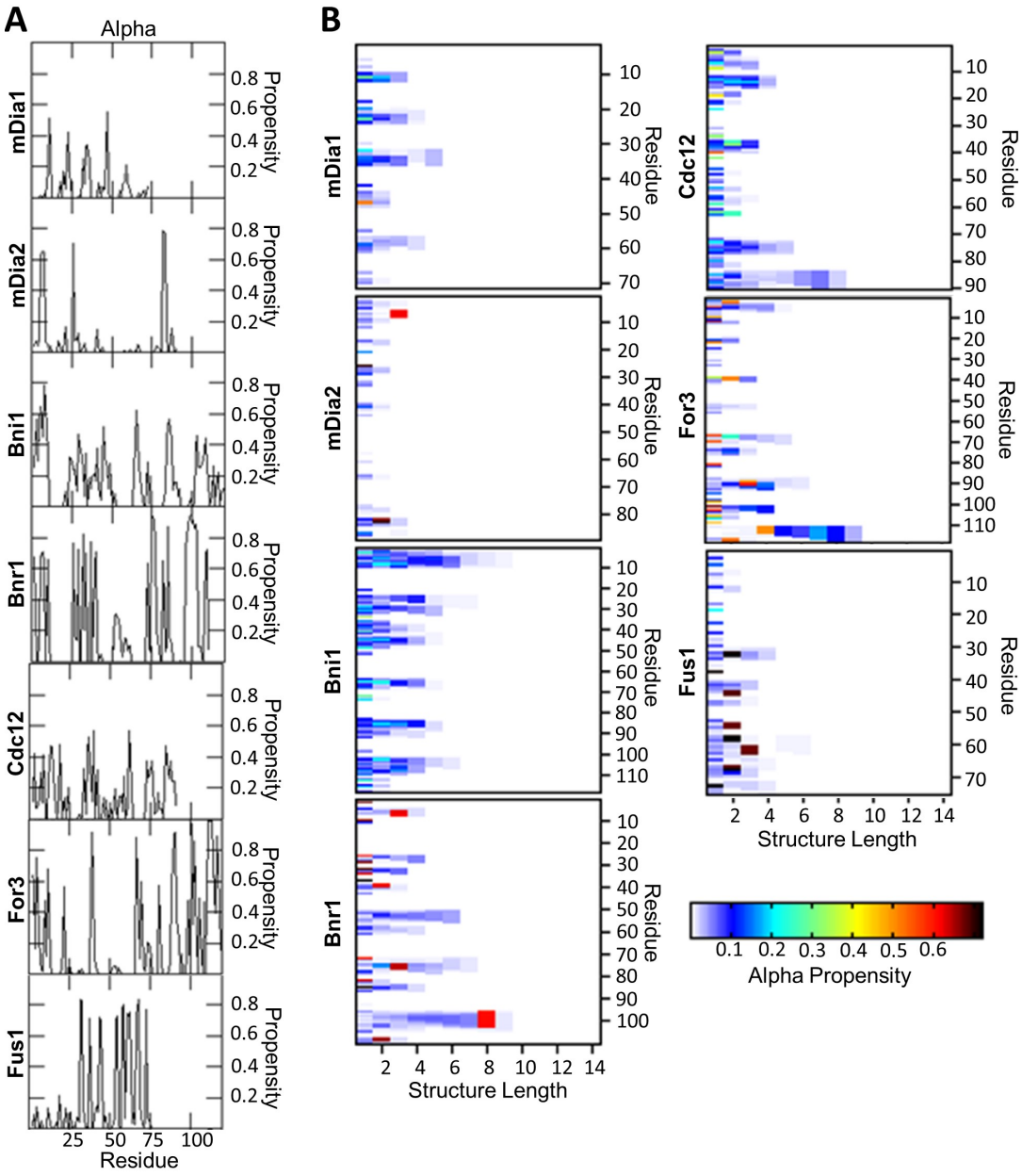

FIGURE S3 **All-atom serial simulations reveal little to no alpha helical structures in the FH1 domain. A**: Total per-residue propensity. **B**: Per-residue and structure length propensity for alpha helices. Secondary structure is classified by backbone dihedral angles.

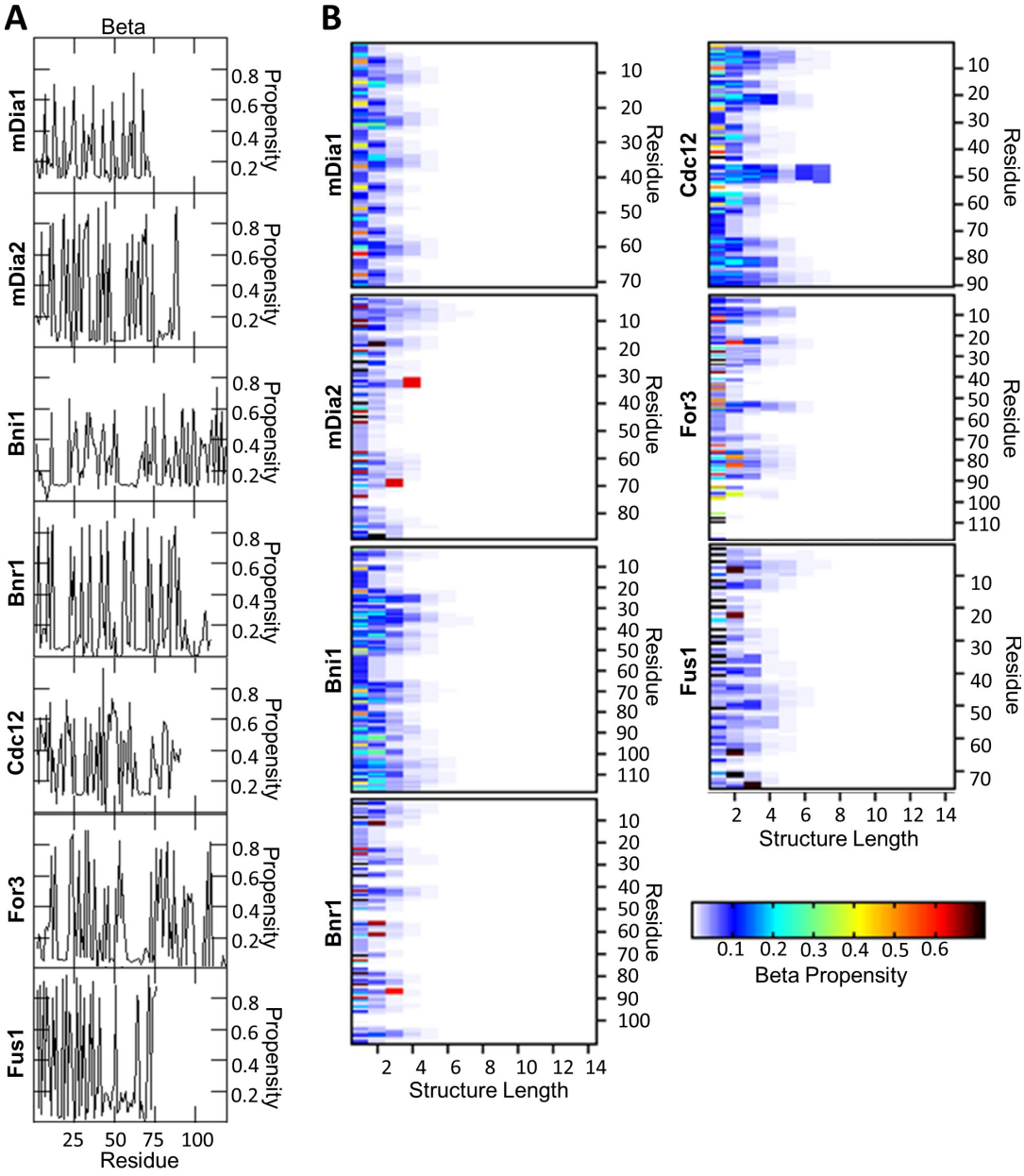

FIGURE S4 **All-atom serial simulations reveal little to no beta type structures in the FH1 domain. A**: Total per-residue propensity. **B**: Per-residue and structure length propensity for beta structures. Secondary structure is classified by backbone dihedral angles.

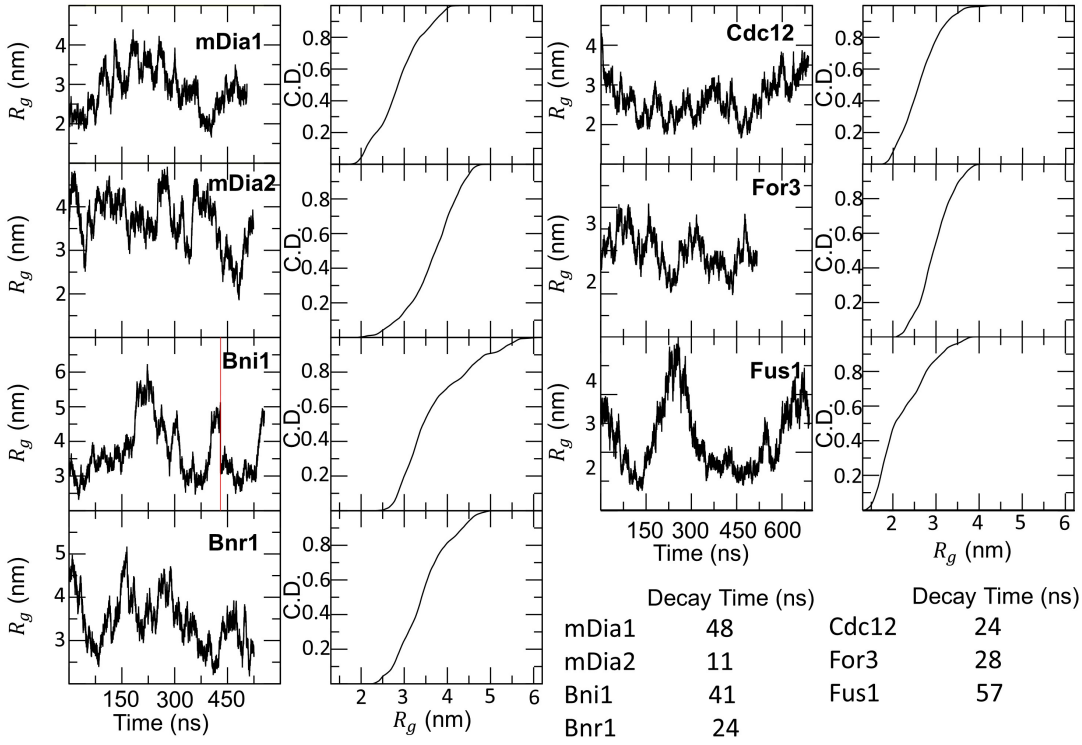

FIGURE S5 R_g **time traces and distributions for the all-atom serial simulations of the FH1 domains showin in Fig. 1A of the main text**. The red line in Bni1 represents where the simulation was cut off and resolvated in a larger box because continuation without this resulted in significant periodic image interaction. Decay times are the first time that the autocorrelation function of R_g drops below $1/e$. Decay time for Bni1 calculated for simulation before resolvated in larger box.

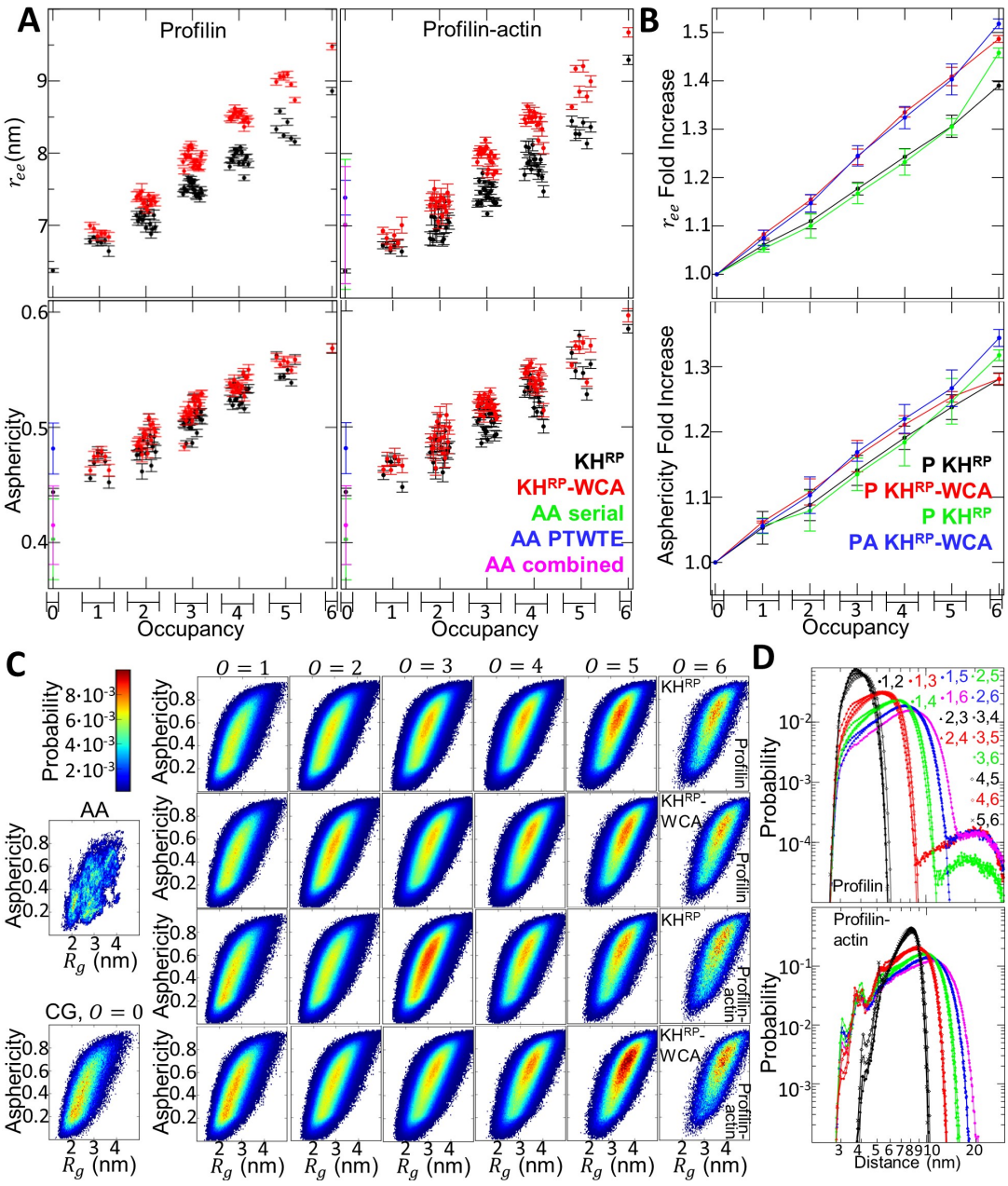

FIGURE S6 **Additional Details on Occupied FH1 Size. A**: Average end to end distance and asphericity, plotted in the same way as for R_g in Figure 4D. **B**: End to end distance and asphericity fold increase, plotted in the same way as for R_g in Figure 4B. **C**: Additional R_g vs. asphercity maps. Left column: unoccupied combined all-atom and unoccupied coarse-grained maps. The 4x6 block shows that R_g and asphericity are always positively correlated over all simulations for a given occupancy for a given model for occupying profilin or profilin-actin. It also shows the the change in the width and location of the peaks of the distribution. **D**: Distance distributions between occupying profilin or profilin-actin. Distributions are over all simulations containing a given pair of occupying profilin or profilin-actin.

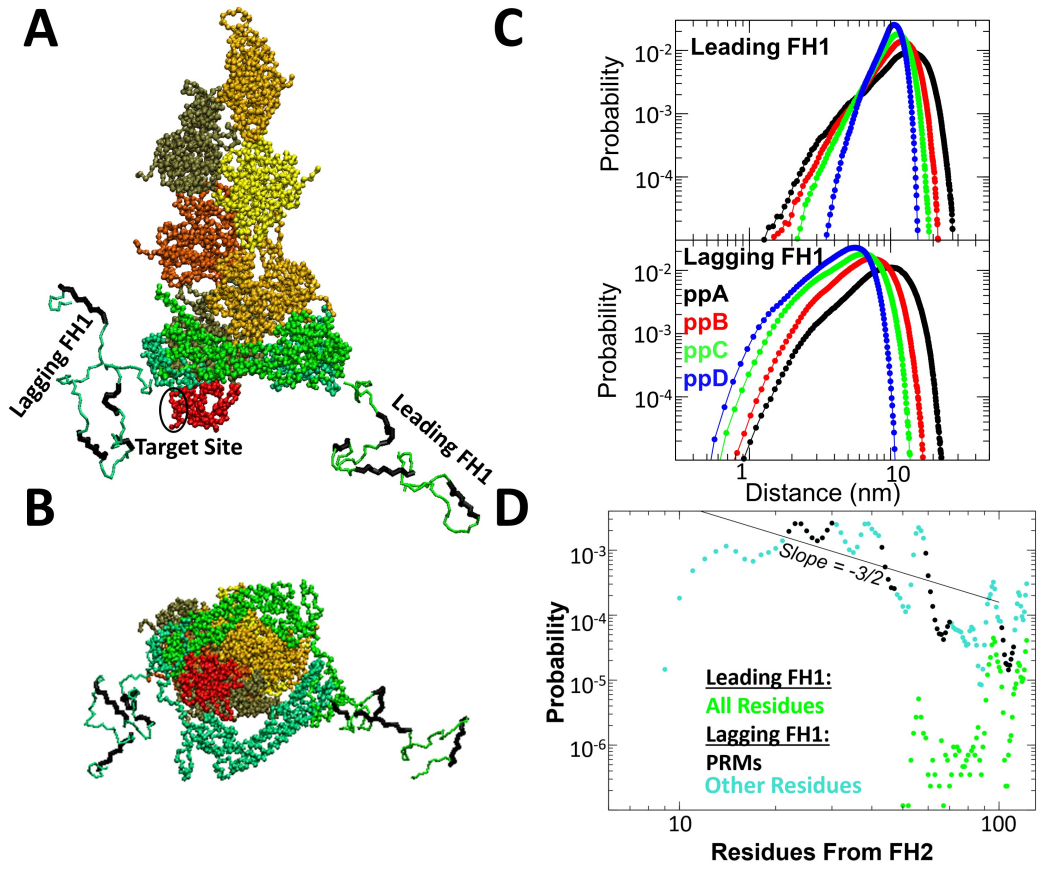

FIGURE S7 **Coarse-grained simulations of FH1 as part of Bni1 FH1-FH2 dimer associated with the barbed end of an actin filament, with one less actin subunit at the barbed end compared to Fig. 5 of the main text. A,B:** Screenshot of typical simulation configuration. This simulation is the same as that of Fig. 5, except that the most-terminal actin subunit has been removed, and profilin placed on the next actin subunit in the filament (i.e. the last subunit on the other protofilament). **C:** Distance distributions of FH1 PRMs to the target site on profilin (same as in Fig. 5) show the lagging FH1 is now favored for closure. **D:** Per-residue probability of closure for each FH1.

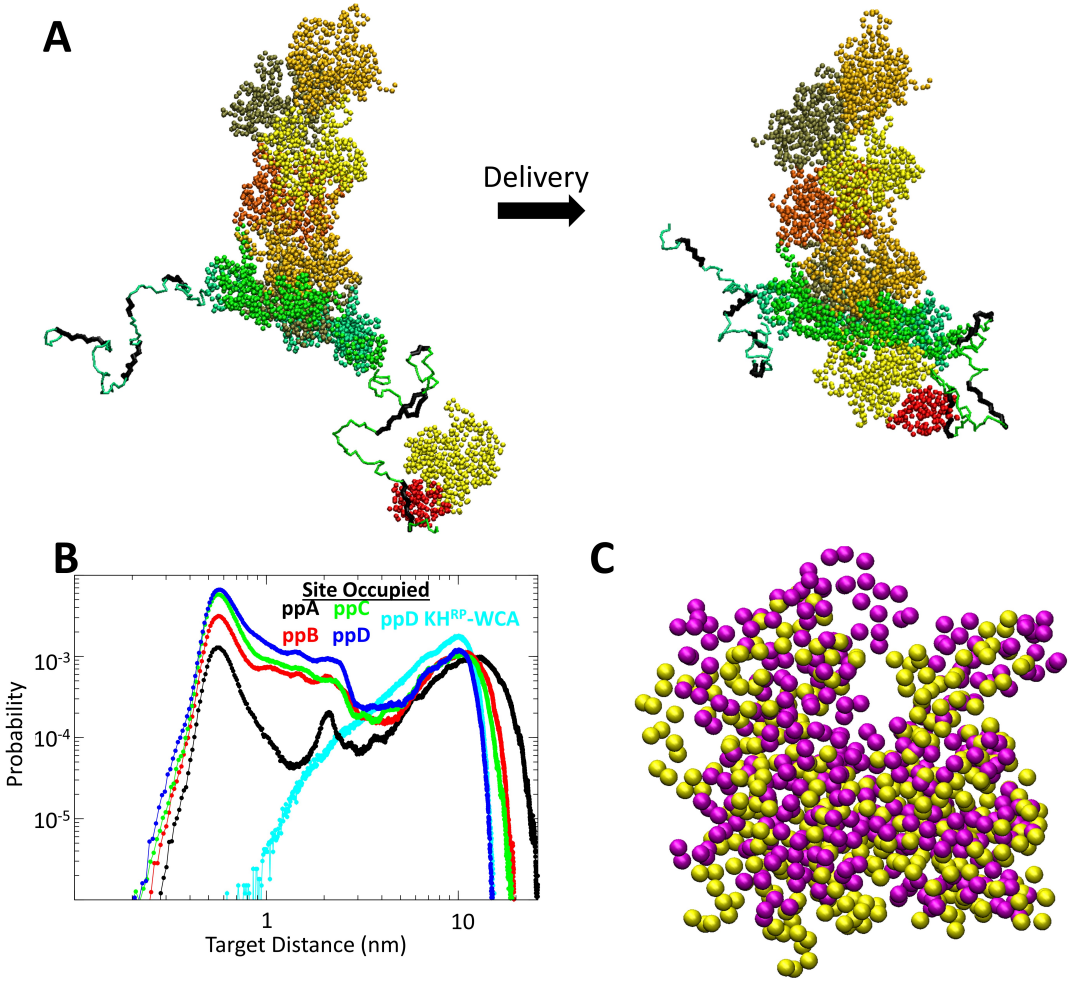

FIGURE S8 **Coarse-grained simulations of FH1 as part of FH1-FH2 dimer associated with the barbed end of an actin filament with profilin-actin bound to the leading FH1. A:** Screenshot of typical simulation configuration in the "far from target" state and in the "close to target" state. These simulations are the same as that of Fig. 5 (total simulation time 80-100 μs), except that the most-terminal actin subunit has been removed and placed on one of the leading FH1 PRMs. In these simulations, we observe multiple transient associations between the incoming actin subunit and the barbed end with duration 10-200 ns (Movie 19). **B:** Distance distributions of profilin-actin bound to each FH1 PRM to the target site on the barbed end. Target distance defined as distance between center of mass of actin bound to profilin-bound FH1 to center of mass of the expected actin delivery site. Features in the distributions near 2 nm correspond to insufficient sampling of profilin-actin bound to FH1 finding the incorrect orientation near the barbed end. Cyan data are for KH-WCA, where there are no attractive interactions between profilin-actin bound to FH1 and the barbed end. **C:** Screenshot overlaying image of actin bound to the profilin-bound FH1 in the "close to target" state (yellow) and image of expected orientation of the next monomer to be delivered after delivery and transfer has occurred (magenta). This result shows that incoming actin transiently docks with the correct orientation for polymerization.